Crack Identification Using Neuro-Fuzzy-Evolutionary Technique

Mun-Bo Shim*
Graduate Student, School of Mechanical Engineering, Sungkyunkwan University
Jangan-Gu, Suwon, Kyungki-Do 440-746, Korea
Myung-Won Suh
Associate Professor, School of Mechanical Engineering, Sungkyunkwan University.,
Jangan-Gu, Suwon, Kyungki-Do 440-746, Korea

It has been established that a crack has an important effect on the dynamic behavior of a structure. This effect depends mainly on the locationanddepthofthecrack.Toidentifythelocation and depth of a crack in a structure, a method is presented in this paper which uses neuro-fuzzy-evolutionary technique, that is, Adaptive-Network-based Fuzzy Inference System (ANFIS) solved via hybrid learning algorithm(the back-propagation gradient descent and the least-squares method) and Continuous Evolutionary Algorithms(CEAs) solving single objective optimization problems with a continuous function and continuous search space efficiently are unified. With this ANFIS and CEAs, it is possible to formulate the inverse problem. ANFIS is used to obtain the input(the location and depth of a crack) - output(the structural Eigenfrequencies) relation of the structural system. CEAs are used to identify the crack location and depth by minimizing the difference from the measured frequencies. We have tried this new idea on beam structures and the results are promising.

Key Words : Crack Identification, Neuro-Fuzzy-Evolutionary Technique, Structure Analysis, Adaptive-Network-Based Fuzzy Inference System; Inverse Analysis Method, Continuous Evolutionary Algorithms

1. Introduction

Techniques to detect cracks and defects hidden in structure and to evaluate their residual life time are very important to assure the structural integrity of operating plants and structures. Many researchers have investigated the potential of system identification to determine the properties of a structure. A state of damage could be detected by a reduction in stiffness. A crack, which occurs in a structural element, causes some local variations in its stiffness which affects the dynamics of the whole structure to considerable degree. An analysis of the changes is tried to identify the crack. Most of the studies on crack identification problem have adopted the modal parameter or the dynamic response to identify the global stiffness and mass matrices of a structure.

A crack in a structure introduces a local flexibility, which is a function of the crack depth. This flexibility changes the stiffness and the dynamic behavior of the structure. Chondros and Dimarogonas (1979, 1980) considered the crack as a local elasticity, which effects the elasticity of the whole cracked structure under consideration and related the crack depth with the frequency decrease. Gounaris and Dimarogonas (1988) have constructed a special cracked beam finite element and Papadopoulos and Dimarogonas (1992) used a 6×6 compliance matrix, including off diagonal terms, to simulate a cracked shaft and to

* Corresponding Author,
E-mail : shimmb@nature.skku.ac.kr
TEL : +82-31-290-7502; **FAX** : +82-31-290-5276
Graduate Student, School of Mech. Eng., Sungkyunkwan Univ., Jangan-Gu, Suwon, Kyungki-Do, 440-746, Korea. (Manuscript **Received** May 25, 2001; **Revised** February 15, 2002)

study its dynamic behavior.

A number of papers deal with the problem of crack location and size identification in order to propose new, efficient and more precise methods. Inagai et al. (1981) used a procedure with eigenfrequency measurements to find the crack size and location. Leung (1992) and Anifantis et al. (1987) proposed crack identification methods through measurements of the dynamic behavior in bending. Dimarogonas and Massouros (1981) investigated the dynamic behavior of a circumferentially cracked shaft in torsion and proposed the nomographs for finding the crack depth and location. Nikolakopoulos et al. (1997) presented the dependency of the structural eigenfrequencies on crack depth and location in contour graph form. To identify the location and depth of a crack, they determined the intersection points of the superposed contours that correspond to the measured eigenfrequency variations caused by the crack presence. However, the intersecting points of the superposed contours are not only difficult to find but also incorrect to evaluate since the procedure mainly depends on men's eye.

The use of neural networks in detecting the damage has been developed for several years, because of their ability to cope with the analysis of the structural damage without the necessity for intensive computation. Neural networks are expected to be a potential approach to detect the damage of the structure (Wu et. al., 1992; Yoshimura and Yagawa, 1993; Tsou and Shen, 1994; Shi et. al., 1999). In these researches, the proposed methods are mostly solving the inverse problem of the identification of the structural damage, that is, mapping problem from vibration characteristics to the structural parameters using the neural network. Because of such a mapping problem, they used a variety of input-output relation, for example, the input is the FFT amplitude of a given range and the output is the structural parameters or the input is the structural eigenfrequencies and modal vectors and the output is the structural parameters. However, it is very expensive to use/calculate these inputs (the 200 input nodes for the FFT amplitude of a given range or many accelerometers for obtaining mode-shape). Also, an approximate estimate is often not good because inverse function is a subset of original input, in fact such a subset could even be empty, so that the usual concept of function breaks down. To identify the location and depth of a crack in a structure with efficient inverse analysis approach and with only eigenfrequency information, hybrid neuro-genetic technique was developed by authors (Suh et. al., 2000). However, it needs to be improved since it is very difficult to obtain the learned network due to the nature of neural network (Jang, 1993; Jang and Sun, 1995).

To identify the location and depth of a crack in a structure with only eigenfrequency information efficiently, a method is presented in this paper which uses neuro-fuzzy-evolutionary technique. Adaptive-Network-based Fuzzy Inference System (ANFIS) (Jang, 1993; Jang and Sun, 1995) solved via hybrid learning algorithm (the back-propagation gradient descent and the least-squares method) are used to obtain the input (the location and depth of a crack)-output (the structural eigenfrequencies) relation of the structural system. With this ANFIS, Continuous Evolutionary Algorithms (CEAs) (Furukawa and Yagawa, 1997), which are efficient in real parameter identification problem, are used to identify the crack location and depth minimizing the difference from the measured frequencies.

2. Inverse Analysis Method

The inverse analysis is generally defined as identifying the parameter set $x^* \in X$ when measured, or reference data $y^* \in Y$ and direct mapping $\psi : X \rightarrow Y$ are known. Problems with the nonlinear direct mapping ψ are termed nonlinear inverse problems. In practice, deterministic models describe reality only in an idealized sense, and thus we may express the input-output relation as follows:

$$y = \psi(x) + \varepsilon \tag{1}$$

where $\varepsilon = \varepsilon_1 + \varepsilon_2$, and ε_1 and ε_2 are errors in the measurement of y and those in the model equations, respectively.

In the analysis of field quantities shown in

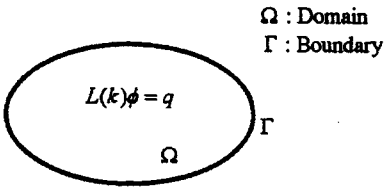

Fig. 1 Problems of field quantities

Fig. 1, the model equations in general take the form:

$$L(k)\,\phi = q \tag{2}$$

where L, k, ϕ, q are the differential operator, material property, field quantity and a source term, respectively.

Inverse problems for Eq. (2) can be classified in terms of the parameter set to be identified: (a) domain Ω, (b) governing equations, (c) boundary conditions, (d) force or source q applying in Ω, (e) material properties k defined in Ω and involved in the governing equations (Furukawa and Yagawa, 1997). In these problems, the input and output vectors reside in the continuous space. There are two main strategies for solving inverse problems. One is to solve a set of equations and the other is to directly find the minimum or maximum of a certain function. However, the former is worth noting the following difficulty: the inverse problem can always be defined as an abstract theoretical concept. In general, inverse function is a subset of original input, in fact such a subset could even be empty, so that the usual concept of "function" as a "one-to-one" injection breaks down. Generally, it is reasonable to solve the latter. Out of them, minimizing a least square criterion has been most widely used for identification.

In this approach, optimization techniques are used to find the input by adjusting them until the measured, or reference data match the corresponding data computed from parameter set in the least square fashion, i.e.

$$\textbf{minimize } f(x) \tag{3a}$$

with the cost functional

$$f(x) = \sum_{i=1}^{m} k_i (y_i^* - \Psi_i(x))^2 \tag{3b}$$

where k_i is a weighting factor. Various calculus-based optimization techniques have been intensively used to solve this optimization problem. These techniques can, however, fail if errors contained in the model equations and in the measurement cause the objective function to be complex. In such cases, the solution may result in a local minimum, unless some regularization method is incorporated. The present study uses genetic algorithm, which is significantly promising for complex optimization.

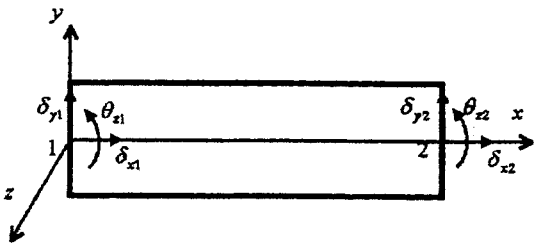

Fig. 2 A beam finite element with extension and bending

3. Structure Analysis

In the finite element model of a damaged structure, the effect of a crack on the behavior of the structure can be simulated through the introduction of the transfer matrices which are method for finding the stiffness matrix. A planar frame structure can be modeled using two-dimensional beam elements having 3 d.o.f. (δ_x, δ_y, θ_z) per node, that is, with extension and bending, in Fig. 2.

The corresponding stiffness and consistent mass local matrices (Pilkey and Wunderlich, 1994) are

$$[K_e] = \frac{EI_{zz}}{L^3}\begin{bmatrix} \beta L^2 & 0 & 0 & -\beta L^2 & 0 & 0 \\ 0 & 12 & 6L & 0 & -12 & 6L \\ 0 & 6L & 4L^2 & 0 & -6L & 2L^2 \\ -\beta L^2 & 0 & 0 & \beta L^2 & 0 & 0 \\ 0 & -12 & -6L & 0 & 12 & -6L \\ 0 & 6L & 2L^2 & 0 & -6L & 4L^2 \end{bmatrix} \tag{4}$$

$$[M_e] = \frac{\rho AL}{420}\begin{bmatrix} 140 & 0 & 0 & 70 & 0 & 0 \\ 0 & 156 & 22L & 0 & 54 & -13L \\ 0 & 22L & 4L^2 & 0 & 13L & -3L^2 \\ 70 & 0 & 0 & 140 & 0 & 0 \\ 0 & 54 & 13L & 0 & 156 & -22L \\ 0 & -13L & -3L^2 & 0 & -22L & 4L^2 \end{bmatrix} \tag{5}$$

where $\beta = A/I_{zz}$, L is the length of element e and

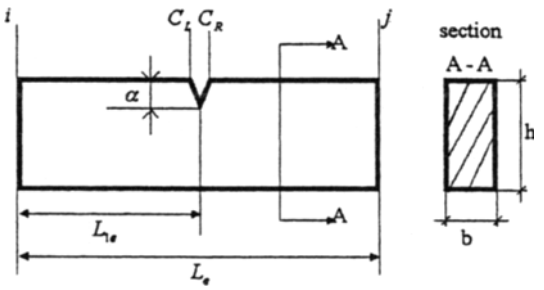

Fig. 3 A cracked beam finite element

L is the cross section area. E and ρ are the modulus of elasticity and mass density, respectively, and I_{zz} is the second moment of inertia about the local z-axis.

From the Euler-Bernoulli theory for the above mentioned degrees of freedom, the transfer matrix [21] which transfers the state variables (displacement, force) from one node to the other node, is

$$[T_e]=\begin{bmatrix} 1 & 0 & 0 & \frac{-L}{AE} & 0 & 0 \\ 0 & 1 & L & 0 & \frac{L^3}{6EI_{zz}} & -\frac{L^2}{6EI_{zz}} \\ 0 & 0 & 1 & 0 & \frac{L^2}{2EI_{zz}} & \frac{L}{EI_{zz}} \\ 0 & 0 & 0 & -1 & 0 & 0 \\ 0 & 0 & 0 & 0 & -1 & 0 \\ 0 & 0 & 0 & 0 & L & -1 \end{bmatrix} \quad (6)$$

A beam finite element of length L_e, containig a crack of depth α at distance L_{1e} from its left end, is depicted in Fig. 3.

The crack introduces a local compliance in the structure. The state vectors at positions i, C_L, C_R, are j are

$$\{z_i\}=\{\delta_{xi}\ \delta_{yi}\ \theta_{zi}\ F_{xi}\ F_{yi}\ M_{zi}\}^T \quad (7a)$$
$$\{z_L\}=\{\delta_{xL}\ \delta_{yL}\ \theta_{zL}\ F_{xL}\ F_{yL}\ M_{zL}\}^T \quad (7b)$$
$$\{z_R\}=\{\delta_{xR}\ \delta_{yR}\ \theta_{zR}\ F_{xR}\ F_{yR}\ M_{zL}\}^T \quad (7c)$$
$$\{z_j\}=\{\delta_{xj}\ \delta_{yj}\ \theta_{zj}\ F_{xj}\ F_{yj}\ M_{zj}\}^T \quad (7d)$$

If no force is acting between nodes i and j, then it can be derived from simple beam theory, where the four state vectors are related as follows:

$$\{z_L\}=[T_1]\{z_i\} \quad (8a)$$
$$\{z_R\}=[T_C]\{z_L\} \quad (8b)$$
$$\{z_j\}=[T_2]\{z_R\} \quad (8c)$$

where $[T_1]$ and $[T_2]$ are the transfer matrices of the subelements C_L-i and C_R-j, respectively

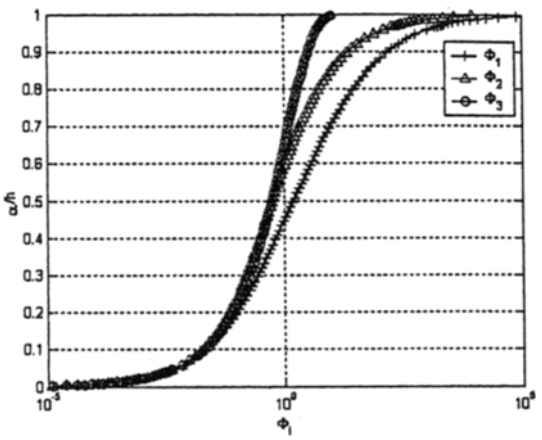

Fig. 4 Φ_i vs α/h for single edge notch specimen under pure tension, bending and shear

$[T_C]$ and is the point transfer matrix due to the crack. Matrix $[T_C]$, which relates the state vectors on the left and right of the crack, is

$$[T_C]=\begin{bmatrix} 1 & 0 & 0 & c_{11} & 0 & c_{13} \\ 0 & 1 & 0 & 0 & c_{22} & 0 \\ 0 & 0 & 1 & c_{31} & 0 & c_{33} \\ 0 & 0 & 0 & -1 & 0 & 0 \\ 0 & 0 & 0 & 0 & -1 & 0 \\ 0 & 0 & 0 & 0 & 0 & -1 \end{bmatrix} \quad (9)$$

where subscripts 1, 2 and 3 correspond to tension, shear and bending, respectively. Terms c_{13} and c_{31}, responsible for the coupling of tension and bending (Gounaris and Dimarogonas, 1988), are not considered here, whereas the rest are known as follows (Papadopoulos and Dimarogonas, 1988):

$$c_{11}=\frac{2(1-\nu^2)\Phi_1}{Eb}, \quad c_{22}=\frac{2k^2(1-\nu^2)\Phi_3}{Eb}, \quad c_{33}=\frac{72(1-\nu^2)\Phi_2}{Ebh^2} \quad (10a\text{-}c)$$

where ν is Poisson's ratio, k is a constant which for rectangular cross sections is known to be 1.5 and Φ_i are functions of the nondimensional crack depth α/h (Papadopoulos and Dimarogonas, 1988). These functions, which are presented in Fig. 4, are integrals of the empirical formulas used by Tada (1973) for computation of stress intensity factors K_I in single edge notch specimens under pure tension, bending and shear.

From Eqs. (8a) ~ (8c) the following is obtained:

$$\{z_j\}=[T_e^C]\{z_i\} \tag{11}$$

The transfer matrix $[T_e^C]$ of the cracked element is written in the form

$$[T_2^C]=[T_2][T_C][T_1]=\begin{bmatrix}A_1 & A_2\\ A_3 & A_4\end{bmatrix} \tag{12}$$

where $[A_i]$ are 3×3 submatrices. Eq. (12) leads to the stiffness matrix of the crack element:

$$[K_e^C]=\begin{bmatrix}-[A_2]^{-1}[A_1] & [A_2]^{-1}\\ [A_3]-[A_4][A_2]^{-1}[A_1] & [A_4][A_2]^{-1}\end{bmatrix} \tag{13}$$

The equation of motion in matrix form is known to be

$$(-\omega^2[M]+[K])\{x\}=\{0\} \tag{14}$$

where ω is eigenfrequency, x is a displacement vector. The above analysis serves to identify the location and depth of a crack in a frame structure, just by measuring the eigenfrequency variations.

4. Neuro-Fuzzy-Evolutionary Technique for Crack Identification

The cracked structure in this study is discretized into a set of elements and the crack is assumed to be located within one of the elements. An ANFIS architecture for the cracked structure is obtained to approximate the response of the structure from the data set prepared through the finite element analysis for various crack sizes and locations. For estimating the location and size of a crack CEAs are utilized, based on the ANFIS architecture. The ANFIS and CEAs are for the so called off-line and on-line function, respectively. The off-line performance is to construct an ANFIS architecture using the input-output pairs including the location and depth of a crack as input and the structural eigenfrequencies as output. The on-line performance is to identify the crack location and depth using CEAs. Neuro-Fuzzy-Evolutionary technique as well as ANFIS and CEAs will be introduced in the following sections, focused on our application.

4.1 Adaptive-network-based fuzzy inference system

Before Adaptive-Network-based Fuzzy Inference System (ANFIS) is introduced, an adaptive network has to be defined. An adaptive network, which is a superset of all kinds of neural network paradigms with supervised learning capability, is a network structure whose overall input-output behavior is determined by the values of a collection of modifiable parameters. More specifically, the configuration of an adaptive network is composed of a set of nodes connected through directed links, where each node is a process unit that performs a static node function on its incoming signals to generate a single node output and each link specifies the direction of signal flow from one node to another. Usually a node function is a parameterized function with modifiable parameters. By changing these parameters, we are actually changing the node function as well as the overall behavior of the adaptive network. The learning rule specifies how these parameters should be changed to minimize the difference from the reference. The basic learning rule of adaptive networks is based the gradient descent method which is notorious for its slowness and tendency to become trapped in local minima. Figure 5 shows typical feed-forward and recurrent adaptive networks with two inputs and two outputs.

A class of adaptive networks that act as a fundamental framework for adaptive fuzzy infer-

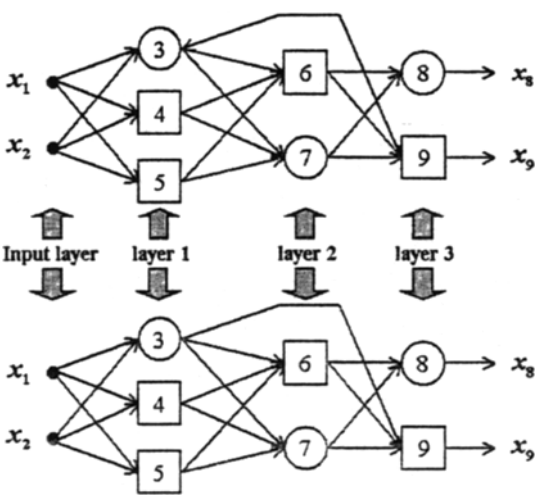

Fig. 5 A recurrent & feed-forward adaptive network in layered representation

ence systems is referred to as "ANFIS" (Jang, 1993), which stands for Adaptive-Network-based Fuzzy Inference System, or semantically equivalently, Adaptive Neuro-Fuzzy Inference System. The ANFIS architecture and its learning algorithm, which is used in this paper, for a first-order Sugeno fuzzy model will be described primarily.

For describing ANFIS architecture in the first place, we assume the fuzzy inference system under consideration has two inputs x, y and one output z. For a first-order Sugeno fuzzy model (Sugeno and Kang, 1998), a typical rule set with two fuzzy if-then rules can be expressed as

Rule 1: If x is A_1 and y is B_1, then
$f_1=p_1x+q_1y+r_1$,

Rule 2: If x is A_2 and y is B_2, then
$f_2=p_2x+q_2y+r_2$

Figure 6(a) illustrates the reasoning mechanism for this Sugeno model. The corresponding equivalent ANFIS architecture is as shown in Fig. 6 (b), where nodes of the same layer have similar functions, as described below. Here we denote the output node i in layer l as $O_{l,i}$.

Layer 1: Every node i in this layer is an adaptive node with a node output defined by

$$O_{1,i}=\mu_{A_i}(x), \text{ for } i=1, 2, \text{ or}$$
$$O_{1,i}=\mu_{B_{i-2}}(x), \text{ for } i=3, 4 \tag{15}$$

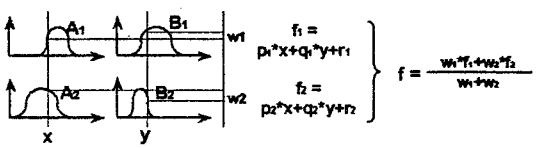

(a)

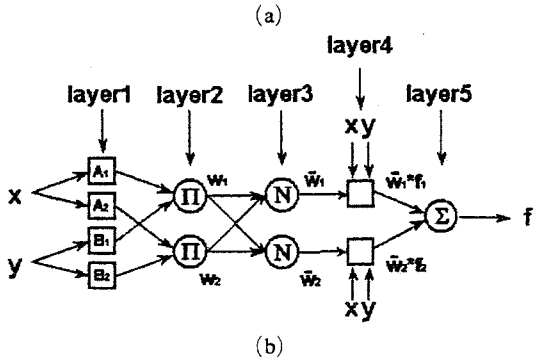

(b)

Fig. 6 (a) A two-input first-order Sugeno fuzzy model with two rules, (b) equivalent

where x (or y) is the input to the node and A_i (or B_{i-2}) is a fuzzy set associated with this node. In other words, outputs of this layer are the membership values of the premise part. Here the membership functions for A_i and B_i can be any appropriate parameterized membership functions. For example, A_i can be characterized by the generalized bell function;

$$\mu_A(x)=\frac{1}{1+\left[\left(\frac{x-c_i}{a_i}\right)^2\right]^{b_i}} \tag{16}$$

where $\{a_i, b_i, c_i\}$ is the parameter set. Parameters in this layer are referred to as premise parameters.

Layer 2: Every node in this layer is a fixed node labeled Π, which multiplies the incoming signals and output the product. For instance,

$$O_{2,i}=w_i=\mu_{A_i}(x)\times\mu_{B_i}(x), \quad i=1, 2 \tag{17}$$

Each node output represents the firing strength of a rule.

Layer 3: Every node in this layer is a fixed node labeled N. The i-th node calculates the ratio of the i-th rule's normalized firing strength to the sum of all rules' firing strengths:

$$O_{3,i}=\bar{w}_i=\frac{w_i}{w_1+w_2}, \quad i=1, 2 \tag{18}$$

Layer 4: Every node in this layer is an adaptive node with a node function

$$O_{4,i}=\bar{w}_if_i=\bar{w}_i(p_ix+q_iy+r_i) \tag{19}$$

where $\bar{w}_i$ is the output of layer 3 and $\{p_i, q_i, r_i\}$ is the parameter set. Parameters in this layer will be referred to as consequent parameters.

Layer 5: The single node in this layer is a fixed node labeled Σ, which computes the overall output a the summation of all incoming signals:

$$O_{5,1}=\text{overall output}=\sum_i\bar{w}_if=\frac{\sum_i w_if_i}{\sum_i w_i} \tag{20}$$

Thus an adaptive network that has exactly the same function as a Sugeno fuzzy model has been constructed. Note that the structure of this adaptive network is not unique; one can easily combine layers 3 and 4 to obtain an equivalent network with only four layers. Figure 7 illustrates an ANFIS of this type.

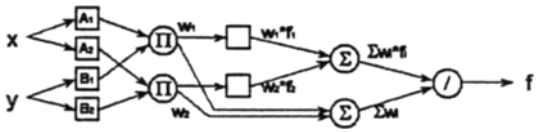

Fig. 7 Another ANFIS architecture for the two-input two-rule Sugeno fuzzy model

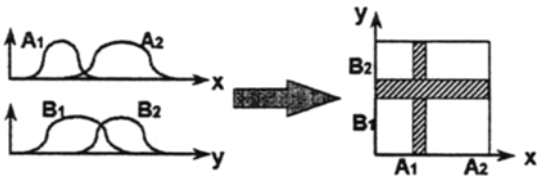

Fig. 8 Partition of the input space into four fuzzy regions

Figure 8 illustrates how the 2-D input space is partitioned into four overlapping fuzzy regions, each of which is governed by fuzzy if-then rules. In other words, the premise part of a rule defines a fuzzy region, while the consequent part specifies the output within this region.

From the ANFIS architecture shown in Fig. 6 (b), we observe that the ANFIS architecture consists of two trainable parameter sets:

1) The antecedent membership function parameter $\{a_i, b_i, c_i\}$.
2) The polynomial parameters $\{p_i, q_i, r_i\}$, also called the consequent parameters.

The ANFIS training paradigm uses a gradient descent algorithm to optimize the antecedent parameters and a least squares algorithm to solve for the consequent parameters. Because it uses two very different algorithms to reduce the error, the training rule is called a hybrid. The consequent parameters are updated first using a least squares algorithm when the values of the premise parameters are fixed and the antecedent parameters are then updated by back-propagating the errors that still exist. Accordingly, the hybrid approach converges much faster since it reduces the dimension of the search space of the original back-propagation method.

4.2 Continuous evolutionary algorithms

Evolutionary algorithms (EAs) are probabilistic optimization algorithm based on the model of

```
k = 0;
Initialize P(k)
do
        Evaluate P(k);
        Select P(k);
        Recombine P(k);
        Mutate P(k);
        k = k +1;
while terminal condition is not satisfied
```

Fig. 9 Fundamental structure of evolutionary algorithms

natural evolution and the algorithm has clearly demonstrated its capability to create good approximate solutions in complex optimization problems. Fig. 9 shows the fundamental structure of evolutionary algorithms.

Continuous evolutionary algorithms (CEAs) (Furukawa and Yagawa, 1997) are one of EAs, which is specifically formulated for the optimization with continuous search space. The reproductive operations of CEAs are intended to be similar to those of genetic algorithms (GAs) such that it can take the advantage of probabilistic features in GAs. The major difference of CEAs from GAs is that a search point itself, i.e. a real continuous vector, gives the representation of the individual. First, a population of individuals, each represented by a continuous vector, is initially (generation $k=0$) generated at random, i.e.,

$$P^k=\{x_1^k, \cdots, x_\lambda^k\}\in(R^n)^\lambda \tag{21}$$

where R^n represents the number of real variables and λ is the number of parental individuals in the problem. Each vector thus represents a search point, which corresponds to the phenomenological representation of individual, that is, the phenotype.

The definition of the recombination and mutation becomes the probabilistic distribution of the phenomenological measures accordingly. The recombination operation is then defined as (Furukawa and Yagawa, 1997; Shim et. al., 2000)

$$\begin{cases} x'_\alpha=(1-\mu_\alpha^k)\,x_\alpha^k+\mu_\beta^k x_\beta^k \\ x'_\beta=\mu_\alpha^k x_\alpha^k+(1-\mu_\beta^k)\,x_\beta^k \end{cases} \tag{22}$$

where x_α^k and k_β^k are parental individuals at generation k and parameter μ_i^k, $\forall i \in \{\alpha, \beta\}$ may be defined by the normal distribution with mean 0 and standard deviation σ

$$\mu_i^k = N(0, \sigma^2) \tag{23}$$

The standard deviation can adopt a self-adaptive strategy (variable with respect to k) or be simply constant. The self-adaptive strategy makes the convergence rate required for each generation faster at the expense of the computation time and vice versa.

The mutation can also be achieved simply by implementing

$$x'' = \text{rand}(x_{\min}, x_{\max}) \tag{23}$$

Note that the mutation may not be necessary since it can allow individuals to alter largely with small possibility, when the coefficient μ_i^k is large.

The evaluation of the fitness can be conducted with a linear scaling, where the fitness of each individual is calculated as the worst individual of the population subtracted from its objective function value

$$\Phi(x_i^k) = \max\{f(x^k) | x^k \in P^k\} - f(x^k), \quad \forall i \in \{1, \cdots, \lambda\} \tag{23}$$

as in GAs. $\Phi(x_i^k) \geq 0$ is thus satisfied by this equation. Proportional selection, which is the most popular selection operation in GAs, also is directly used in CEAs as it requires $\Phi(x_i^k) \geq 0$. The reproduction probabilities of individuals $p_s : X \rightarrow [0, 1]$ are given by their relative fitness,

$$p_s(x_i^k) = \frac{\Phi(x_i^k)}{\sum_{j=1}^{\lambda} \Phi(x_j^k)} \geq 0 \tag{24}$$

Optionally, ranking selection can be implemented in this algorithm. These reproductive operations form one generation of the evolutionary process, which corresponds to one iteration in the algorithm, and the iteration is repeated until a given terminal criterion is satisfied.

4.3 Neuro-fuzzy-evolutionary technique for crack identification

For the crack identification, it is known that crack parameters such as the location and depth of a crack can be determined from the measured eigenfrequencies of structure. This can be classified as the inverse problem. In this study, neuro-fuzzy-evolutionary technique is adopted to identify the crack parameters in a structure.

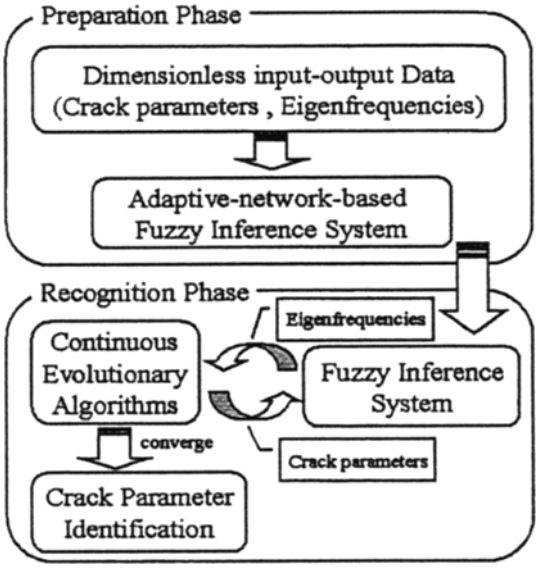

Fig. 10 Crack identification procedure on neuro-fuzzy-evolutionary technique

Overall procedure of this study is shown in Fig. 10. There are preparation phase and recognition phase. In the preparation phase, the learning data of various sets of dimensionless crack parameters and the corresponding response of the structure, which is the dimensionless eigenfrequency change in this study, are prepared by the computational structure analysis which is presented in sec. 3 of this paper. The ANFIS architecture described in subsection 4.1 is adopted to approximate the response of the cracked structure from the prepared learning data.

In the recognition phase, the parameters which identify the crack are estimated by CEAs described in subsection 4.2 using the ANFIS architecture obtained in the preparation phase. Using the ANFIS architecture, crack identification problem can be constructed in terms of optimization with CEAs. The optimization problem to be formulated is defined as follows

$$\underset{\alpha^*, L_1^*}{\text{Min}} F(\alpha^*, L_1^*) = \sum_{i=1}^{3} w_i (\Omega_i - \Omega_i^*)^2 \tag{25}$$
$$\alpha^{*lower} \leq \alpha^* \leq \alpha^{*upper}, \; L_1^{*lower} \leq L_1^* \leq L_1^{*upper}$$

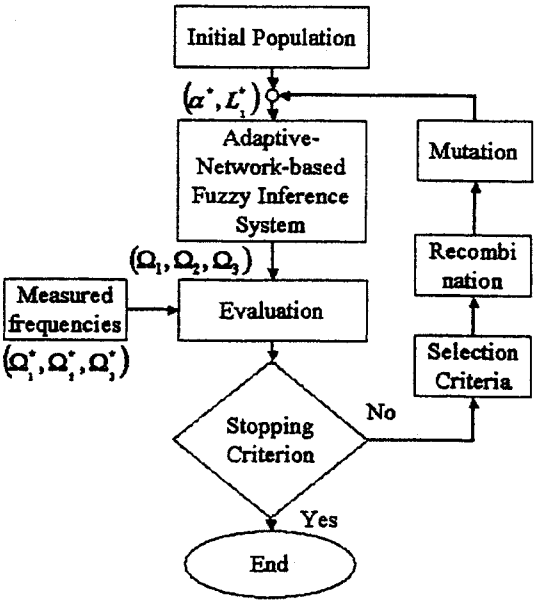

Fig. 11 Flowchart of the neuro-fuzzy-evolutionary technique

where α^*, L_1^*, is the dimensionless depth and location of a crack, w_i is a weighting factor and Ω_i is the dimensionless eigenfrequency which is functions ofα^* and L_1^*; and Ω_i^* is the dimensionless measured or reference eigenfrequency. The general procedure is illustrated in Fig. 11.

5. Numerical Simulation

The clamped-free beam of Fig. 12 has a length of L=3m, rectangular cross section $B \times H$= 0.2m×0.2m and contains a crack of depth α at a distance L_1 from the clamped end. The material properties are $E=2.07\times10^{11}\mathrm{Nm}^{-2}$, ν=0.3, and ρ=7700kgm^{-3}. The beam is discretized into 12 two-node finite elements. For the ANFIS architecture, 10 sets of a crack depth α=0.01m, 0.02m, ···, 0.1m (step size=0.01m) are introduced at the 29 different locations L_1=0.1m, 0.2m, ···, 2.9m (step size=0.1m). Totally 290 cases or patterns (10 different crack depths and 29 different crack locations) are solved for the first three eigenfrequencies. The nondimensional crack depth $\alpha^*=\alpha/H$ and crack location $L_1^*=L_1/L$ as well as the dimensionless eigenfrequency change $\Omega_i=1-f_{c\_i}/f_{u\_i}$ will be used. Subscripts u and c

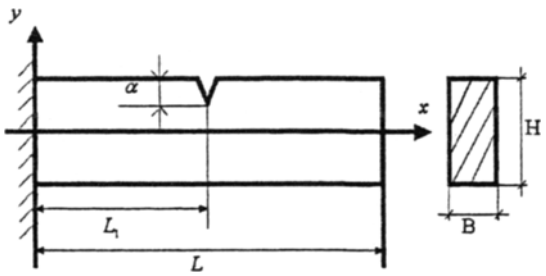

Fig. 12 Model of the cracked clamped-free beam

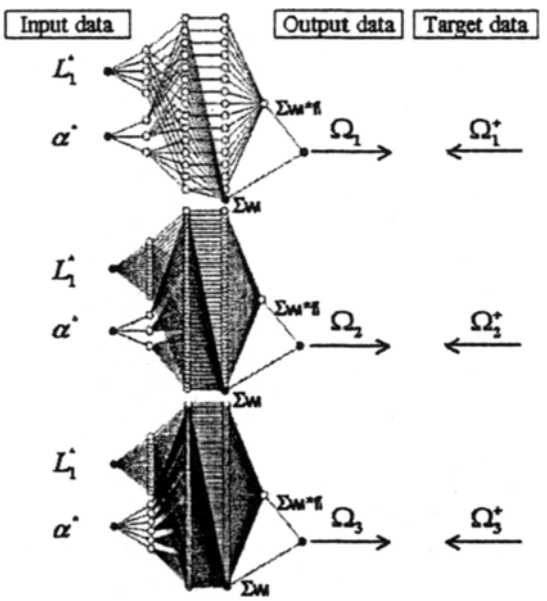

Fig. 13 Three ANFIS architecture for a two-input first-order Sugeno fuzzy model with 15 rules, 42 rules and 90 rules, respectively

denote results for the uncracked and cracked beams, respectively. The first three eigenfrequencies of the uncracked beam are obtained (f_{u_1}= $117 rad/s$, f_{u_2}=$732 rad/s$, f_{u_3}=$2029 rad/s$) solving Eq. (14) except the crack matrix. The patterns which consist of 290 sets of data are used to train three ANFIS architecture of Fig. 13. Through some trials, rules in Fig. 13 are concluded to be the best for our application. In addtion, to update the antecedent parameters by back-progating the errors, the adaptive learning rate is used. That is, if the error decreases the learning rate is increased by 1.1. Otherwise, the learning rate is decreased by 0.9.

Root Mean Squared Error(RMSE) is empolyed

as a measuremenet of modeling performance. The mathematical expression can be described as follows:

$$RMSE=\frac{\sqrt{\sum_{i=1}^{N}(e_i)^2}}{N} \tag{26}$$

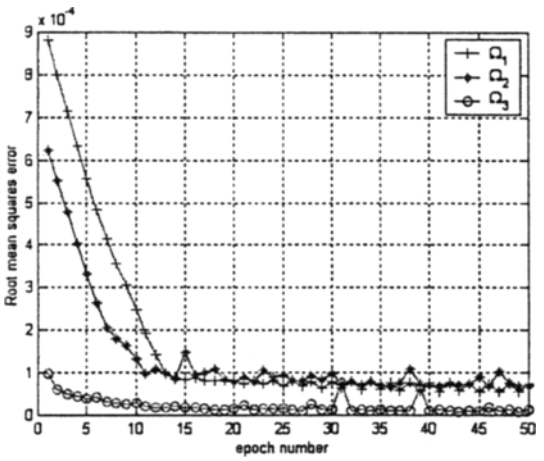

Fig. 14 RMSE curves for three ANFISs

where e_i denotes an error at pattern i and N is the total number of pattern. Figure 14 shows the RMSE curves for three ANFIS which indicate most of the learning was done in the 50 epochs, respectively. The final RMSE is 6.45e-3, 4.92e-2, 1.84e-2, respectively when the RMSE not of dimensionless eigenfrequencies change but of crack eigenfrequencies is calculated and total RMSE is 5.5e-2.

The estimated crack eigenfrequencies from the ANFIS architecture are compared to the target values as shown in Fig. 15. In order to check the ANFIS architecture, 9 sets of a crack depth α= 0.015m, 0.025m, ···, 0.095m (step size=0.01m) are introduced at the 28 different locations L_1= 0.15m, 0.25m, ···, 2.85m (step size=0.1m). Totally unlearning 252 cases or patterns(9 different crack depths and 28 different crack locations) are compared to the exact values as shown in Fig. 16 and then total RMSE is 3.2479. This result shows that the ANFIS architecture is well learned.

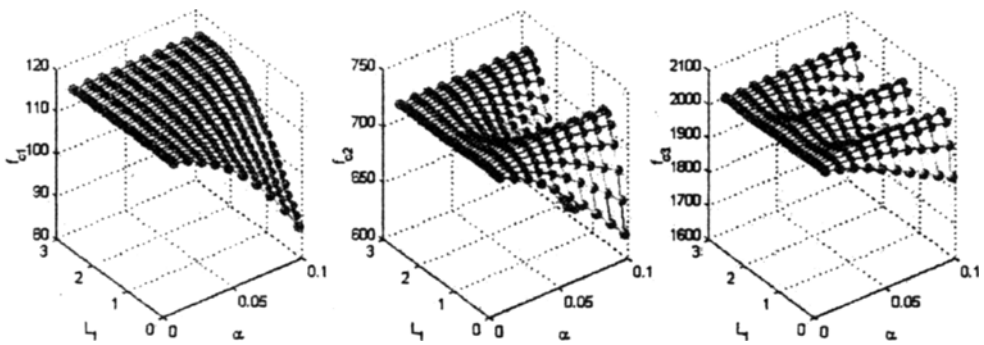

Fig. 15 Comparison of the estimated eigenfrequencies from the ANFIS architecture to target values (o : target value, * : estimated value)

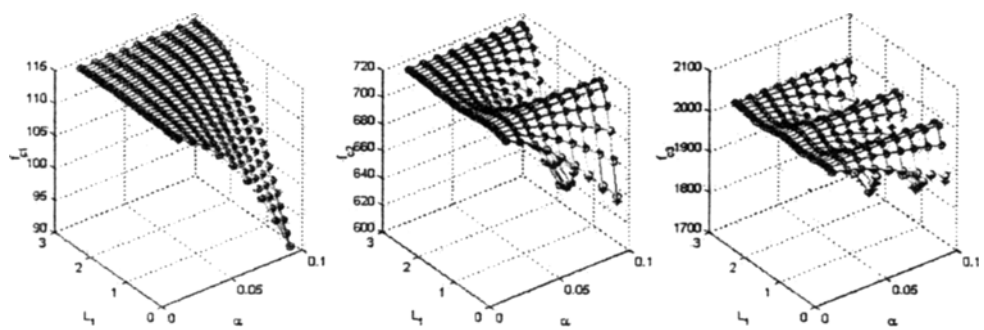

Fig. 16 Comparison of the unlearning eigenfrequencies from the ANFIS architecture to target values (o : target value, * : estimated value)

Table 1 Crack identification result: Clamped-free beam

	Case (a)		
	Reference value	Result value	Relative Error(%)
$\alpha^*(\alpha)$	0.1(0.02)	0.099(0.020)	1.0(1.4)
$L_1^*(L_1)$	0.1(0.30)	0.097(0.310)	3.0(3.0)
$\Omega_1(f_{c\_1})$	0.030(113.48)	0.031(113.35)	3.3(0.11)
$\Omega_2(f_{c\_2})$	0.024(714.46)	0.024(714.23)	1.3(0.03)
$\Omega_3(f_{c\_3})$	0.011(2007.56)	0.011(2007.62)	0.3(0.01)
	Case (b)		
	Reference value	Result value	Relative Error(%)
$\alpha^*(\alpha)$	0.325(0.065)	0.322(0.064)	0.1(0.1)
$L_1^*(L_1)$	0.35(1.05)	0.357(1.071)	1.9(1.9)
$\Omega_1(f_{c\_1})$	0.061(109.83)	0.056(110.45)	8.6(0.57)
$\Omega_2(f_{c\_2})$	0.049(696.24)	0.048(697.12)	2.5(0.12)
$\Omega_3(f_{c\_3})$	0.025(1910.72)	0.058(1909.97)	5.8(0.04)

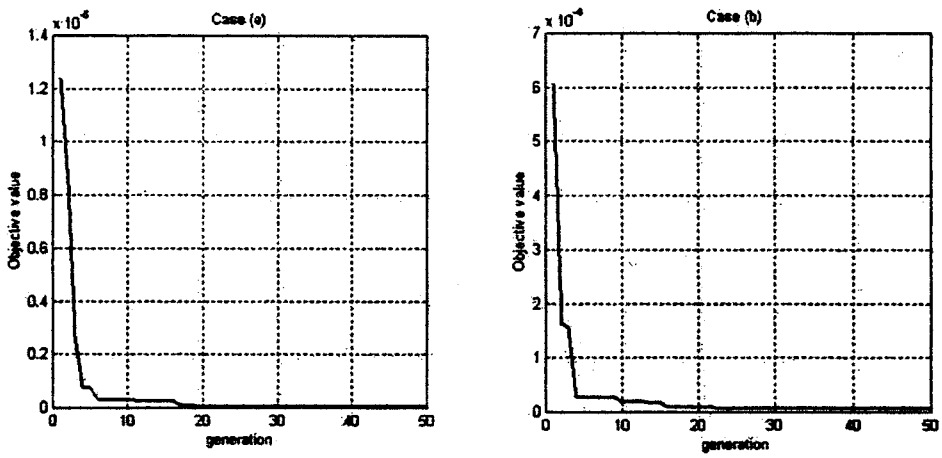

Fig. 17 Generation history of Case (a) and Case (b)

Because the ANFIS architecture obtained above can be adopted to approximate the response of the cracked structure, the parameters which identify the crack are estimated by CEAs. Using the ANFIS architecture, crack identification problem can be constructed from Eq. (25). Then CEAs for this study is set-up: population size, $N=50$; standard deviation, $\sigma=0.5$; mutation rate, $M=0.02$. Also, proportional selection method is adopted for the selection process.

The clamped-free beam of Fig. 12 is adopted as an example problem, two cases are considered. (a) A crack of depth α of 0.02 m exists at L_1 of 0.3 m. The first three eigenfrequencies are obtained computationally based on the theory described in section 3: $f_{c\_1}=113.48 rad/s$, $f_{c\_2}=714.46 rad/s$, $f_{c\_3}=20007.56 rad/s$. (b) A crack of depth of 0.065 exists at of 1.05. The first three eigenfrequencies are obtained computationally based on the theory described in section 3: $f_{c\_1}=109.83 rad/s$, $f_{c\_2}=696.24 rad/s$, $f_{c\_3}=1910.72 rad/s$.

The neuro-fuzzy-evolutionary technique has been applied to this example problem. Figure 17 illustrates convergence history of the objective function for case (a) and case (b), respectively. The searches meet the convergence after 19 and 22 iterations for case (a) and case (b), respectively.

Table 2 Comparison of Neuro-Fuzzy-Evolutionary technique to Hybrid neuro-genetic technique

	Neuro-Fuzzy-Evolutionary technique		Hybrid Neuro-Genetic technique	
	ANFIS		Back-Prop. NN	
Training Data	290		290	
RMSE	0.055		5.26	
Epoch Number	503		100,000	
	CEAs		GAs	
	Case (a)	Case (b)	Case (a)	Case (b)
Generation No. of Optimal Sol.	19	22	84	47

The result of Table 1 shows that the location and depth of a crack are estimated by the neuro-fuzzy-evolutionary technique within 3% error. Also, the corresponding eigenfrequencies are very close to the reference values within 0.6% error.

Table 2 lists the general performance of both neuro-fuzzy-evolutionary technique and hybrid neuro-genetic technique, which were measured by using each method to predict 290 points immediately following the training set and to identify the location and depth of a crack for two cases. The RMSE obtained through back-propagation neural network is 5.26 which is much worse than that of the ANFIS architecture. Also, CEAs incorporating continuous representation of points demonstrate its convergence faster than that of GAs.

6. Conclusions

A methodology of neuro-fuzzy-evolutionary technique for the crack identification from the eigenfrequencies is proposed based on the fact that a crack has an important effect on the dynamic behavior of a structure. To estimate the crack parameters adaptive-network-based fuzzy inference system and continuous evolutionary algorithm are combined into the proposed technique. The ANFIS architecture is for the approximation of the eigenfrequencies as the functions of the crack parameters and the CEAs is for finding crack parameters which minimize the difference from the measured eigenfrequencies.

The effectiveness of this technique is confirmed by a example problem. The crack parameters of the clamped-free beam problem are estimated within 3% error. It can be concluded that good agreements are obtained between the depth and location of the estimated crack and that of the reference one.

The neuro-fuzzy-evolutionary technique can be generalized for general boundary condition and structure to estimate the crack location and depth provided that the reference data, or training data to learn the ANFIS architecture are properly prepared.

Acknowledgements

The authors are grateful for the support provided by a grant from the Korea Science & Engineering Foundation (KOSEF) and Safety and Structural Integrity Research Center at the Sungkyunkwan University.

References

Anifantis, N., Rizos, P. and Dimarogonas, A. D., 1987, "Identification of Cracks on Beams by Vibration Analysis," *In: 11th Biennial ASME Conf. on Mechanical Vibration and Noise*, Boston.

Chondros, T. C. and Dimarohonas, A. D., 1979, "Identification of Cracks in Circular Plates Welded at the Contour," *In: ASME Design Engineering Technical Conf.*, St. Louis.

Chondros, T. C. and Dimarogonas, A. D., 1980, "Identification of Cracks in Welded Joints of Complex Structures," *Journal of Sound and Vi-*

bration, 69, pp. 531~538.

Dimarogonas, A. D. and Massouros, G., 1981, "Torsional Vibrations of a Shaft with a Circumferential Crack," *Engineering Fracture Mechanics*, 15, pp. 439~444.

Furukawa, T. and Yagawa, G., 1997, "Inelastic Constitutive Parameter Identification Using an Evolutionary Algorithm with Continuous Individuals," *International Journal for Numerical Methods in Engineering*, Vol. 40, pp. 1071~1090.

Gounaris, G. D. and Dimarogonas, A. D., 1988, "A Finite Element of a Cracked Prismatic Beam in Structural Analysis," *Computational Structure*, 28, pp. 309~313.

Gounaris, G. D. and Papazoglou, V., 1992, "Three-Dimensional Effects on the Natural Vibration of Cracked Timoshenko Beams in Water," *Computational Structure* 42, pp. 769~779.

Inagaki, T., Kanki, H. and Shiraki, K., 1981, "Transverse Vibrations of a General Cracked Rotor Bearing System," *Journal of Mechanical Design*, 104, pp. 1~11.

Jang, J.-S. R., 1993, "ANFIS: Adaptive-Network-Based Fuzzy Inference Systems," *IEEE Transactions on Systems, Man and Cybernetics*, Vol. 23, No. 3, pp. 665~685.

Jang, J.-S. R. and Sun, C.-T., 1995, "Neuro-Fuzzy Modeling and Control," *Proceedings of the IEEE*.

Leung, P. S., 1992, "The effects of a Transverse Crack on the Dynamics of a Circular Shaft," *In: Rotordynamics'92. Int. Conf. on Rotating Machine Dynamics, Venice*.

Nikolakopoulos, H. G., Katsareas, D. E. and Papadopoulos, C. A., 1997, "Crack Identification in Frame Structures," *Computer & Structures*, Vol. 64, No. 1-4, pp. 389~406.

Papadopoulos, C. A. and Dimarogonas, A. D., 1988, "Coupled Longitudinal and Bending Vibrations of a Cracked Shaft," *Journal of vibrational acoustics stress reliability design*, 110, pp. 1~8.

Pilkey, W. D. and Wunderlich, W., 1994, *Mechanics of Structures Variational and Computational Methods*, Boca Raton: CRC press.

Sugeno, M. and Kang, G. T., 1998, "Structure Identification of Fuzzy Model," *Fuzzy Sets and System*, Vol. 28, pp. 15~33.

Shi, Q., Hagiwara, I. and Sekine, T., 1999, "Structural Damage Detection and Identification Using Learning Vector Quantization Neural Network," *Proceeding of the ASME Design Engineering Technical Conference*.

Suh, M.-W., Shim, M.-B. and Kim, M.-Y., 2000, "Crack Identification Using Hybrid Neuro-Genetic Technique," *Journal of Sound and* Vibration, 238(4), pp. 617~635.

Shim, M.-B., Furukawa, T., Yoshimura, S., Yagawa, G. and Suh, M.-W., 2000, "Efficient Multi-Point Search Algorithms for Multiobjective Optimization Problem," *Proceedings of Conference on Computational Engineering and Science*, Vol. 5, No. 2, pp. 459~462.

Tada, H., 1973, *The Stress Analysis of Cracks Handbook*, Del Research Corporation. PA.

Tsou, P. and Shen, M.-H., 1994, "Structural Damage Detection and Identification Using Neural Network," *AIAA Journal*, Vol. 32, No. 1, pp. 176~183.

Wu, X., Ghaboussi J. and Garrett, J. H., 1992, "Use of Neural Networks in Detection of Structural Damage," *Computer & Structures*, Vol. 42, No. 4, pp. 649~659.

Yoshimura, S. and Yagawa, G., 1993, "Inverse Analysis by Means of Neural Network and Computational Mechanics: its Application to Structural Identification of Vibrating Plate," *Inverse Problems*, pp. 184~193.

Appendix

To give the readers a concrete idea of the resulting fuzzy inference systems, it would be better to show the change of membership functions (in Fig. 18) and to list the fuzzy if-then rules explicitly. Here we list the final 15 fuzzy if-then rules of the first eigenfrequency in example problem 1 which predicts the eigenfrequencies of the clamped-free beam. Suppose that the input a^* is assigned three linguistic values SMALL, MEDIUM and LARGE and the input L^* is assigned five linguistic values VERY SHORT, SHORT, HALF, LONG, VERY LONG, then the fuzzy if-then rules after training can be expressed as:

$$
\begin{cases}
\text{If } \alpha^* \text{ is } SMALL \text{ and } L_1^* \text{ is } VERY\ SHORT, \text{ then } \Omega_1 = c_1 \cdot X \\
\text{If } \alpha^* \text{ is } SMALL \text{ and } L_1^* \text{ is } SHORT, \text{ then } \Omega_1 = c_2 \cdot X \\
\text{If } \alpha^* \text{ is } SMALL \text{ and } L_1^* \text{ is } HALF, \text{ then } \Omega_1 = c_3 \cdot X \\
\text{If } \alpha^* \text{ is } SMALL \text{ and } L_1^* \text{ is } LONG, \text{ then } \Omega_1 = c_4 \cdot X \\
\text{If } \alpha^* \text{ is } SMALL \text{ and } L_1^* \text{ is } VERY\ LONG, \text{ then } \Omega_1 = c_5 \cdot X \\
\text{If } \alpha^* \text{ is } MEDIUM \text{ and } L_1^* \text{ is } VERY\ SHORT, \text{ then } \Omega_1 = c_6 \cdot X \\
\text{If } \alpha^* \text{ is } MEDIUM \text{ and } L_1^* \text{ is } SHORT, \text{ then } \Omega_1 = c_7 \cdot X \\
\text{If } \alpha^* \text{ is } MEDIUM \text{ and } L_1^* \text{ is } HALF, \text{ then } \Omega_1 = c_8 \cdot X \\
\text{If } \alpha^* \text{ is } MEDIUM \text{ and } L_1^* \text{ is } LONG, \text{ then } \Omega_1 = c_9 \cdot X \\
\text{If } \alpha^* \text{ is } MEDIUM \text{ and } L_1^* \text{ is } VERY\ LONG, \text{ then } \Omega_1 = c_{10} \cdot X \\
\text{If } \alpha^* \text{ is } LARGE \text{ and } L_1^* \text{ is } VERY\ SHORT, \text{ then } \Omega_1 = c_{11} \cdot X \\
\text{If } \alpha^* \text{ is } LARGE \text{ and } L_1^* \text{ is } SHORT, \text{ then } \Omega_1 = c_{12} \cdot X \\
\text{If } \alpha^* \text{ is } LARGE \text{ and } L_1^* \text{ is } HALF, \text{ then } \Omega_1 = c_{13} \cdot X \\
\text{If } \alpha^* \text{ is } LARGE \text{ and } L_1^* \text{ is } LONG, \text{ then } \Omega_1 = c_{14} \cdot X \\
\text{If } \alpha^* \text{ is } LARGE \text{ and } L_1^* \text{ is } VERY\ LONG, \text{ then } \Omega_1 = c_{15} \cdot X
\end{cases} \tag{27}
$$

where $X=[\alpha^*\ L_1^*\ 1]$ and c_i is the i-th row of the following consequent parameter matrix C:

$$
c = \begin{bmatrix}
0.331 & 0.02865 & 0.02193 \\
-0.07464 & 0.01993 & 0.01125 \\
-0.06105 & 0.01158 & 0.01138 \\
-0.00138 & 0.006203 & 0.01485 \\
0.0006746 & 0.002138 & 0.01747 \\
0.485 & -0.1557 & -0.01448 \\
0.006172 & -0.1128 & 0.09603 \\
-0.06677 & -0.0697 & 0.08847 \\
0.0003775 & -0.03413 & 0.04682 \\
0.0006231 & -0.01119 & 0.03176 \\
0.9643 & -0.4322 & -0.1825 \\
0.474 & -0.2719 & 0.02079 \\
0.1262 & -0.1275 & 0.07911 \\
-0.007641 & -0.02121 & 0.04297 \\
-0.001608 & 0.003531 & 0.01758
\end{bmatrix} \tag{28}
$$

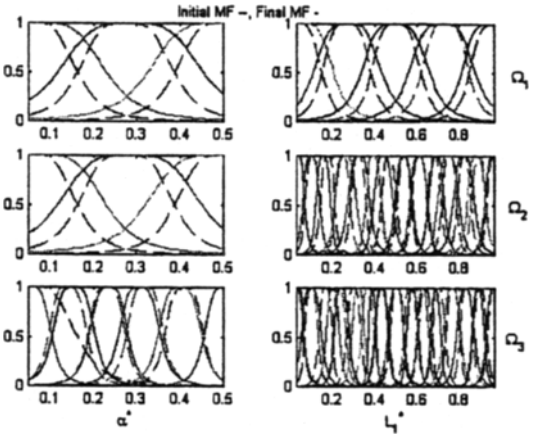

Fig. 18 Membership functions before & after learning, respectively